Table I. Atom Coordinates ($\times 10^4$) and Thermal Parameters ($Å^2 \times 10^3$)

atom	*x*	*y*	*z*	U^a
Cl	1752 (1)	−636 (1)	7152 (1)	54 (1)
S	897 (1)	3140 (1)	7272 (1)	37 (1)
Na	2638 (1)	6562 (1)	5474 (1)	41 (1)
O(1)	−1426 (2)	3278 (3)	7322 (1)	47 (1)
O(2)	1575 (3)	4693 (3)	6795 (1)	57 (1)
O(3)	3650 (3)	4279 (2)	4227 (1)	44 (1)
O(4)	−1048 (2)	8062 (2)	5253 (1)	41 (1)
O(5)	3321 (3)	8568 (2)	4013 (1)	44 (1)
N	2370 (3)	1421 (3)	6695 (1)	42 (1)
C(1)	1561 (3)	2903 (3)	8498 (2)	38 (1)
C(2)	3513 (4)	3165 (5)	8714 (2)	69 (1)
C(3)	4009 (5)	2915 (6)	9681 (2)	82 (2)
C(4)	2634 (4)	2450 (4)	10434 (2)	58 (1)
C(5)	708 (5)	2226 (5)	10203 (2)	71 (1)
C(6)	171 (4)	2432 (5)	9238 (2)	61 (1)
C(7)	3205 (7)	2187 (7)	11492 (3)	94 (2)

[a] Equivalent isotropic *U* defined as one-third of the trace of the orthogonalized U_{ij} tensor.

Table II. Important Bond Distances (Å) and Angles (deg)

N-Cl	1.750 (2)	Na-O(4)	2.357 (2)
N-S	1.590 (2)	Na-O(3)	2.437 (2)
S-O(1)	1.455 (2)	Na-O(5)	2.487 (2)
S-O(2)	1.439 (2)	Na-Cl″	3.153 (1)
S-C(1)	1.767 (2)	O(1)···H(3a)′	2.11 (3)
Na-O(2)	2.365 (2)	O(1)···H(5a)′	2.16 (3)
Cl-N-S	110.9 (1)	O(1)-S-O(2)	116.1 (1)
N-S-C(1)	109.6 (1)	O(1)-S-C(1)	105.8 (1)
O(1)-S-C(1)	105.8 (1)	O(2)-S-C(1)	103.3 (1)
S-O(2)-Na	157.0 (1)	O(2)-S-N	103.6 (1)

entity shown in Figure 1 is the dominant motif and can be roughly described as an aquo-bridged sodium dimer (Na-O = 2.354 (2), 2.437 (2) Å). In addition to the bridging water molecules, the halves of the dimer are held together by a hydrogen bond between a coordinated water molecule and the amido nitrogen (depicted by dotted lines). The sixth coordination site on each sodium is occupied by the chlorine of a neighboring dimer, obtained by a unit translation along *b* (Na···Cl = 3.153 (1) Å).

A different dimer, related by inversion, provides additional hydrogen bonds to N, O(1), O(4), and O(3). Thus, each hydrogen belonging to a water molecule is involved in some type of hydrogen bonding, while each water oxygen, as well as the nitrogen atom, has two hydrogen-bonded contacts. In addition, O(1), a sulfonyl oxygen, has two hydrogen bonds, but O(2) has none, as it is involved in coordination to the sodium. The "N-sodio" interaction is clearly a misnomer, at least in the solid state. The closest N···Na distance is 4.095 (2) Å, and it involves the nitrogen bonded to the coordinated chlorine. Furthermore, the octahedral set of five oxygens and one chlorine surrounding each sodium precludes the close approach of a nitrogen atom.

The N-Cl distance of 1.750 (2) Å equals the mean N-Cl distance in NCl_3(s)[8] and is the same as one of the distances in $[PtCl(NH_3)_3(NCl_2)_2]Cl$ (1.75 (2), 1.66 (2) Å).[9] The S-O(1) and S-O(2) distances are 1.455 (2) and 1.439 (2) Å, which are well within the range of those reported for similar molecules. The slightly longer S-O(1) bond length is presumably due to hydrogen bonding to O(1) but not O(2). The octahedral geometry around sodium is fairly regular. The five Na-O bonds range from 2.354 (2) to 2.487 (2) Å, and the largest deviation from idealized octahedral angles is 103.5 (1)° for O(3)-Na-O(4). This geometry is comparable to that found in sodium acetylacetonate monohydrate.[10] The toluene group is quite normal, with mean ring C-C bonds of 1.377 (4) Å and an average deviation from the mean of 0.009 Å.

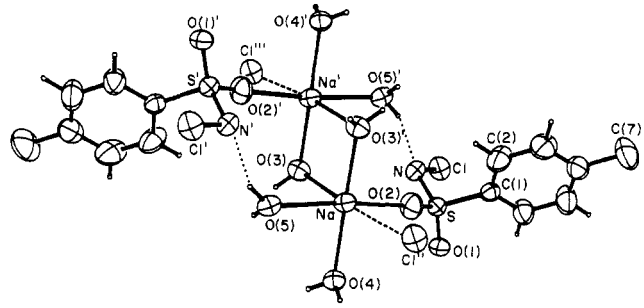

Figure 1. A computer-generated drawing of a portion of the structure of chloramine-T. Anisotropic thermal ellipsoids are shown at the 50% probability level. Centrosysmmetric dimers result from the bridging of sodium by water and from intradimer hydrogen bonds (dotted lines). In addition, the sixth coordination site on each sodium is filled by the chlorine of an adjacent dimer (dashed lines).

To our knowledge, the structure of the RSO_2NCl^- grouping is reported here for the first time. Support of formulation B for the structure of its sodium salt comes from three major structural features: (i) the only interaction between sodium and the SO_2N moiety involves an Na-O rather than an Na-N contact; (ii) the S-N distance, 1.590 (2) Å, is consistent with a double rather than a single bond;[11] (iii) aggregation is a result of the tendency of the Na^+ ion to achieve 6-coordination, which it does through coordination to one sulfonyl oxygen only; two bridging and two terminal waters and a chlorine from another chloramine-T molecule comprise the rest of the coordination sphere. This in turn gives rise to several hydrogen-bonding contacts between water hydrogens and oxygen and nitrogen atoms. Clearly then the aggregation seems to have no significant effect on the structure of the $[4\text{-}MeC_6H_4SO_2NCl]^-$ ion.

In summary, the best description of chloramine-T is that its structure is close to that depicted in B rather than its more common representation A.

Acknowledgment. We thank the Committee on Research of the University of California at Davis for financial support.

Registry No. Chloramine-T trihydrate, 7080-50-4.

Supplementary Material Available: Tables of bond distances and angles, hydrogen bonding interactions, hydrogen coordinates, and anisotropic thermal parameters (3 pages); a list of observed and calculated structure factors (14 pages). Ordering information is given on any current masthead page.

(8) Jander, J. *Adv. Inorg. Chem. Radiochem.* **1976**, *19*, 1-63.
(9) Zipprich, M.; Pritzkow, H.; Jander, J. *Angew. Chem., Int. Ed. Engl.* **1976**, *15*, 225-226.
(10) Sahbari, J. J.; Olmstead, M. M. *Acta Crystallogr. Sect. C: Cryst. Struct. Commun.* **1983**, *C39*, 1037-1038.
(11) Greenwood, N. N.; Earnshaw, A. *Chemistry of the Elements*; Pergamon: New York, 1984; pp 854-881.

Contribution from the Department of Chemistry, The University of Texas at Austin, Austin, Texas 78712

Reversible Addition of CO to a Rh_3 Cluster: Synthesis and X-ray Crystal Structure of $Rh_3(\mu\text{-}t\text{-}Bu_2P)_3(\mu\text{-}CO)(CO)_4$

Richard A. Jones* and Thomas C. Wright

Received May 1, 1986

Facile reversible addition of carbon monoxide to transition-metal clusters is an interesting phenomenon that is relevant to many homogeneous and heterogeneous catalytic reactions.[1] We report here the synthesis and X-ray crystal structure of $Rh_3(\mu\text{-}t\text{-}$

(1) See for example: Farrugia, L. J.; Green, M.; Hankey, D. R.; Orpen, A. G.; Stone, F. G. A. *J. Chem. Soc., Chem. Commun.* **1983**, 310-312. Schneider, J.; Minelli, M.; Huttner, G. *J. Organomet. Chem.* **1985**, *294*, 75-89 and references therein.
(2) Cotton, F. A.; Wilkinson, G. *Advanced Inorganic Chemistry*, 4th ed.; Wiley: New York, 1980; Chapter 30, p 1265.

0020-1669/86/1325-4058$01.50/0

Scheme I

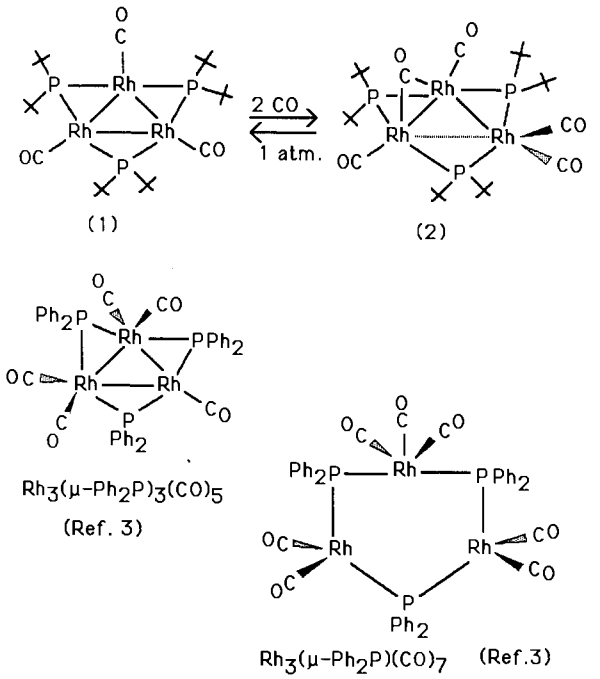

$Bu_2P)_3(\mu\text{-}CO)(CO)_4$ (**2**), which is formed by the reversible addition of 2 mol of CO to 1 mol of $[Rh(\mu\text{-}t\text{-}Bu_2P)(CO)]_3$. **2** is of interest for a number of reasons. In many cases of CO addition to a transition-metal cluster, metal–metal bonds are cleaved.[1] In this case, 2 mol of CO is added to 1 mol of the Rh_3 framework, which expands significantly, but the Rh–Rh bonds do not break completely. One CO now bridges a Rh–Rh bond, and the Rh atom opposite bears two CO units in a roughly tetrahedral geometry (see Scheme I). Of related interest is the diphenylphosphido-bridged Rh_3 system $Rh_3(\mu\text{-}Ph_2P)_3(CO)_x$ (x = 5–9) recently reported by Haines et al.[3] (Scheme I). For these complexes, reversible CO addition has also been observed. However, the structural parameters for $Rh_3(\mu\text{-}Ph_2P)_3(CO)_5$ are strikingly different from those of **2**. These differences are discussed below.

Results and Discussion

Exposure of hexane or THF solutions of $[Rh(\mu\text{-}t\text{-}Bu_2P)(CO)]_3$ (**1**) to CO (1 atm) results in a rapid and dramatic color change from deep red to deep green. If hexane solutions are concentrated by bubbling CO through them and cooled to −40 °C, deep green crystals of $Rh_3(\mu\text{-}t\text{-}Bu_2P)_3(\mu\text{-}CO)(CO)_4$ (**2**) may be isolated in high yield. The compound has a metallic red/green luster in the solid state but appears bright green when crushed. The reaction is readily reversible in solution. Thus, deep green solutions of **2** rapidly lose CO under vacuum, and **1** is re-formed. Crystals of **2** slowly lose CO under a nitrogen atmosphere and more rapidly under vacuum. No further addition of CO can be achieved by exposure of **2** to higher pressures of CO (750 psi).

The IR spectrum of **2** has a band in the bridging CO region (1832 m cm^{-1}), while the $^{31}P\{^1H\}$ NMR spectrum in toluene-d_8 at ambient temperature consists of a broad multiplet at δ 48.08. When the sample is cooled to −80 °C, two complex multiplets are observed at δ 110.65 and 169.72 of relative areas 2:1. Since the room-temperature multiplet does not appear at the weighted average of the low-temperature signals, a simple averaging process in a fluxional molecule at higher temperatures is ruled out. The data suggest a molecule in which there is little significant Rh–Rh bonding at room temperature, while the low-temperature spectrum is consistent with the solid-state structure determined by X-ray crystallography.

The molecular framework of **2** is shown in Figure 1, and key bond lengths and angles are given in Table I. The unique bridging CO unit sits well out of the Rh_3 plane. Thus, the dihedral angle between the Rh3–CO31–Rh1 and Rh1–Rh2–Rh3 planes is 89.3°. The coordination about Rh2 is also of interest since the additional CO molecule gives it a roughly tetrahedral geometry, which is relatively rare for four-coordinate Rh(I).[4] Interestingly, the two Rh–Rh bonds not bridged by CO have lengthened considerably when compared to those observed in **1**. Thus Rh2–Rh3 = 3.021 (1) Å and Rh1–Rh2 = 3.014 (1) Å, while Rh1–Rh3 = 2.779 (1) Å. In the starting complex **1**, the Rh–Rh distances are similar and much shorter (2.649 Å average).[5]

Although the Rh–Rh distances have lengthened significantly, they are still within the upper limits that are generally considered typical of Rh–Rh single bonds. The reversible expansion and contraction of the Rh_3 framework associated with the absorption of two CO molecules is an intriguing process since no bonds are completely broken. The molecular geometry of the Ph_2P-bridged analogue, $Rh_3(\mu\text{-}Ph_2P)_3(CO)_5$, is quite different from that of **2**. In this case, there are no bridging CO ligands; two Rh atoms each

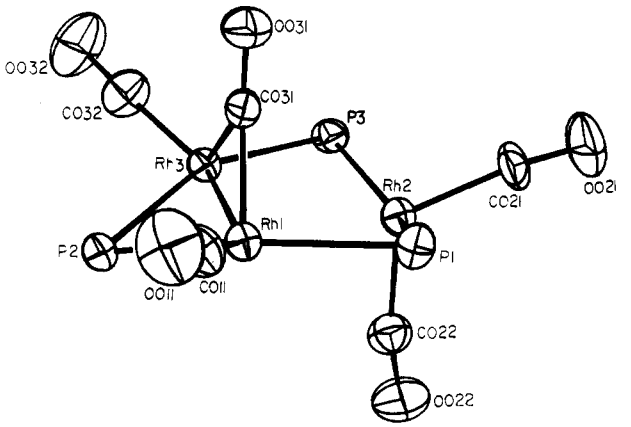

Figure 1. ORTEP view of the central framework of **2**. *tert*-Butyl groups have been omitted for clarity.

Table I. Selected Bond Lengths and Angles for **2**[a]

	Distances, Å		
Rh1–Rh2	3.014 (1)	Rh2–P3	2.338 (1)
Rh2–Rh3	3.021 (1)	Rh2–CO21	1.848 (4)
Rh1–Rh3	2.779 (1)	Rh2–CO22	1.892 (4)
Rh1–P1	2.336 (1)	Rh3–P2	2.338 (1)
Rh1–P2	2.351 (1)	Rh3–P3	2.351 (1)
Rh1–CO11	1.848 (4)	Rh3–CO31	1.974 (4)
Rh1–CO31	1.992 (4)	Rh3–CO32	1.874 (5)
Rh2–P1	2.338 (1)		
	Angles, deg		
Rh3–Rh1–P1	110.90 (3)	Rh2–P3–Rh3	80.22 (3)
Rh3–Rh1–P2	53.43 (2)	Rh1–P2–Rh3	72.70 (3)
Rh3–Rh1–CO11	144.0 (1)	CO21–Rh2–CO22	112.5 (2)
Rh3–Rh1–CO31	45.3 (1)	Rh1–Rh3–P2	53.86 (3)
P1–Rh1–P2	158.70 (4)	Rh1–Rh3–P3	111.37 (3)
P1–Rh1–CO11	97.8 (1)	Rh1–Rh3–CO31	45.8 (1)
P1–Rh1–CO31	95.2 (1)	Rh1–Rh3–CO32	141.0 (1)
P2–Rh1–CO11	102.5 (1)	P2–Rh3–P3	156.71 (4)
P2–Rh1–CO31	82.6 (1)	P2–Rh3–CO31	83.3 (1)
CO11–Rh1–CO31	113.1 (2)	P2–Rh3–CO32	99.7 (1)
P1–Rh2–P3	146.00 (4)	P3–Rh3–CO31	98.0 (1)
P1–Rh2–CO21	95.7 (1)	P3–Rh3–CO32	101.5 (1)
P1–Rh2–CO22	101.7 (1)	CO31–Rh3–CO32	110.7 (2)
P3–Rh2–CO21	96.4 (1)	Rh1–P1–Rh2	80.32 (3)
P3–Rh2–CO22	102.7 (1)		

[a] Numbers in parentheses are estimated standard deviations in the least significant digits.

(3) Haines, R. J.; Steen, N. D. C. T.; English, R. B. *J. Chem. Soc., Dalton Trans.* **1984**, 515.

(4) Kang, S. K.; Albright, T. A.; Wright, T. C.; Jones, R. A. *Organometallics* **1985**, *4*, 666–675. Gaudiello, J. G.; Wright, T. C.; Jones, R. A.; Bard, A. J. *J. Am. Chem. Soc.* **1985**, *107*, 888–897. Jones, R. A.; Wright, T. C.; Atwood, J. L.; Hunter, W. E. *Organometallics* **1983**, *2*, 470–472.

(5) Atwood, J. L.; Hunter, W. E.; Jones, R. A.; Wright, T. C. *Inorg. Chem.* **1983**, *22*, 993–995.

bear two terminal CO's and are bridged by a Ph_2P^- unit that lies well out of the Rh_3 plane. The remaining Rh atom bears a single CO, and the two other μ-Ph_2P groups also lie in the Rh_3 plane. The Rh–Rh distances in this complex are all relatively short with respect to the elongated ones found in **2** (2.793 (1), 2.698 (1), and 2.806 (1) Å). It is only with the heptacarbonyl derivative $Rh_3(\mu\text{-}Ph_2P)_3(CO)_7$ that the Rh–Rh distances becomes comparable with those in **2** (3.124 (11), 3.223 (12), and 3.084 (11) Å).

Experimental Section

All preparative chemistry was performed with standard inert-atmosphere techniques. Solvent preparation and NMR and IR spectra/instrumentation were as previously described.[4] Reliable microanalytical data for **2** could not be obtained due to the loss of CO (see text). $[Rh(\mu\text{-}t\text{-}Bu_2P)(CO)]_3$ (**1**) was prepared as previously described.[5] CO used was CP grade.

Preparation of $Rh_3(\mu\text{-}t\text{-}Bu_2P)_3(\mu\text{-}CO)(CO)_4$ (2). A deep red solution of $[Rh(\mu\text{-}t\text{-}Bu_2P)(CO)]_3$ (**1**) (0.20 g) in hexane (30 mL) was exposed to CO (1 atm) in a glass Schlenk vessel (5 min). The solution became an intense dark green and was concentrated (10 mL) by bubbling CO (1 atm) through it (*hood*). Cooling (−40 °C) for 12 h under a CO atmosphere (1 atm) gave dark crystals of **2** in quantitative yield. Crystals of **2** were isolated by decanting the supernatant liquid under a CO atmosphere. It may be stored at room temperature under a CO atmosphere but reverts slowly to **1** under vacuum or nitrogen in the solid state. **1** is re-formed rapidly by placing solutions of **2** under vacuum, and the cycle is reproducible. Mp: **2** loses CO at 100–105 °C, and the remaining material melts at 223–225 °C [the melting point of $[Rh(\mu\text{-}t\text{-}Bu_2P)(CO)]_3$ (**1**)]. IR (Nujol mull, KBr plates) (cm^{-1}): ν(CO) 1963 m, 1945 s, 1915 w, 1832 m. ^1H NMR (in C_6D_6, ambient temperature relative to Me_4Si, δ 0.0): δ 1.45 (m, t-Bu_2P). $^{31}P\{^1H\}$ NMR (toluene-d_8, relative to 85% H_3PO_4(aq), δ 0.0): at ambient temperature δ 48.08 (m); at −80 °C δ 110.65 (m), 169.72 (m) (relative areas 2:1).

X-ray Crystal Structure of $Rh_3(\mu\text{-}t\text{-}Bu_2P)_3(\mu\text{-}CO)(CO)_4$ (2). Data were collected on an Enraf-Nonius CAD-4 diffractometer using graphite-monochromated Mo Kα radiation. Data were collected by the $\omega/2\theta$ scan technique at 23 ± 2 °C. Details of the standard data collection methods are similar to those outlined in ref 6. All calculations were performed on a PDP 11/44 computer using the Enraf-Nonius software package SDP PLUS.[7] Crystals of **2** were grown from hexane solutions under a CO atmosphere at (−40 °C). These were mounted in thin-walled glass capillaries under nitrogen (1 atm). Unit cell parameters were determined from 25 carefully centered reflections ($26.0° > 2\theta > 30.0°$). Crystal data for **2**: dark green prisms with metallic luster, maximum crystal dimensions 0.24 × 0.25 × 0.28 mm, triclinic, $P\bar{1}$ (No. 2), $C_{29}H_{54}O_5P_3Rh_3$, M_r = 884.39, a = 11.578 (1) Å, b = 11.749 (1) Å, c = 15.502 (1) Å, α = 98.815 (1)°, β = 94.457 (1)°, γ = 117.070 (2)°, V = 1829.3 (5) Å^3, D_c = 1.606 g cm^{-3}, Z = 2, λ(Mo Kα) = 0.710 73 Å (graphite monochromator), μ = 14.786 cm^{-1}; scan width (0.8 + 0.35 tan θ)°; range of indices (hkl) 0 to +13, −13 to +9, −18 to +18; standard reflections $4\bar{3}8$, $2\bar{7}\bar{1}$; decay of standards 9.8%. Data were corrected for Lorentz and polarization effects, and linear decay correction was applied. The structure was solved using MULTAN,[8] followed by successive cycles of difference Fourier maps and then least-squares refinement. All non-hydrogen atoms were refined anisotropically; hydrogen atoms were not located. A non-Poisson contribution weighting scheme with an experimental instability factor P[9] was used in the final stages of refinement (P = 0.04). Full-matrix least-squares refinement of 5258 reflections [$I > 3\sigma(I)$] out of 6082 unique observed ($3.0 < 2\theta < 50.0$) gave R and R_w values of 0.0336 and 0.0567, respectively. Number of variables = 361, data/parameter ratio = 14.565, shift to error ratio = 2.479, and esd of an observation of unit weight = 2.1356. The highest peak in the final difference Fourier was 0.667 e Å^{-3}. Supplementary material is available.[10]

Acknowledgments. We thank the National Science Foundation (Grant CHE 8517759), the Robert A. Welch Foundation (Grant F-816), and the Texas Advanced Technology Research Program for financial support. We also thank Johnson Matthey Inc. for a generous loan of $RhCl_3 \cdot xH_2O$, and R.A.J. thanks the Alfred P. Sloan Foundation for a fellowship (1985–1987).

Registry No. **1**, 104114-25-2; **2**, 104114-26-3.

Supplementary Material Available: A complete ORTEP diagram of **2** and complete listings of bond lengths, angles, positional parameters, and temperature factors (8 pages); a complete listing of structure factors (53 pages). Ordering information is given on any current masthead page.

(6) Jones, R. A.; Wright, T. C. *Organometallics* **1983**, *2*, 1842–1895.
(7) SDP-PLUS (4th ed., 1981): B. A. Frenz and Associates, College Station, TX 77840.
(8) Germain, G.; Main, P.; Wolfson, M. M. *Acta Crystallogr., Sect. A: Cryst. Phys., Diffr., Theor. Gen. Crystallogr.* **1971**, *A27*, 368.
(9) P is used in the calculation of $\sigma(I)$ to downweight intense reflections in the least-squares refinement. The function minimized was $\sum w(|F_o| - |F_c|)^2$ where $w = 4(F_o)^2/[\sum(F_o)^2]_2$, where $[\sum(F_o)^2]^2 = [S^2(C + R^2B) + [P(F_o)^2]^2]/Lp^2$, where S is the scan rate, C is the total integrated peak count, R is the ratio of scan time to background counting time, B is the total background count, and Lp is the Lorentz–polarization factor.
(10) See paragraph at end of paper regarding supplementary material.

Contribution from the Departament de Química, Universitat Autônoma de Barcelona, Bellaterra, 08071 Barcelona, Spain, and Institut "Jaume Almera", CSIC C. Marti Franquês s/n. Ap. Correos, 30102 Barcelona, Spain

Metal Complexes with Polydentate Sulfur-Containing Ligands. Crystal Structure of (2,6-Bis((ethylthio)methyl)pyridine)dibromozinc(II)

Francesc Teixidor,*† Lluis Escriche,† Jaume Casabó,† Elias Molins,‡ and Carlos Miravitlles‡

Received December 18, 1985

The chemistry of transition-metal tridentate ligands containing N and/or O or tetradentates containing N and S as donor atoms is well known and documented, as indicated by the extensive studies on terpyridine (terpy),[1] pyridyl diimines,[2] N_2S_2 macrocycles,[3] or N_2S_2 open-chain ligands.[4] Quinquedentate ligands containing N and/or O have been less studied, probably due to the low availability of compounds of this kind; however, some ligands do exist such as 6,6″-bis(α-methylhydrazino)-4′-phenyl-2,2′:6′,2″-terpyridine = L, whose pentadenticity has been corroborated in $[SnMe_2L][PF_6]Cl$.[5] On the contrary, no structural information is available on tridentate NS_2 (S = thioether) and obviously on quinquedentate $N_xS_2O_{3-x}$ ligands. During the course of writing this paper, we became aware of a very recent paper by Lehn, Parker, and Rummer[6] in which are reported a ligand with the same NS_2 functionalities and its complexes with Rh and Pd, characterized only by spectroscopic methods.

In the course of studies on polynucleating macrocyclic sulfur-containing ligands derived from the condensation of 2,6-bis(bromomethyl)pyridine with thiol derivatives, it was found advantageous to examine the coordination chemistry of some related acyclic ligands. Here we describe the synthesis of a few of these ligands, their metal complexes, and the crystal structure of Zn(IIa)Br_2. To the best of our knowledge, there are only two other structural analyses of similar five-coordinate Zn complexes with one tridentate ligand and two monodentate ligands that have been reported in the literature. These have been reported by Einstein and Penfold[7] for Zn(terpy)Cl_2 and by Petersen, McCormick, and Nicholson[8] for $Zn(dapdH_2)Cl_2 \cdot H_2O$ where $dapdH_2$ is 2,6-diacetylpyridine dioxime. This, indeed, is the first example of a fully characterized complex with a tridentate acyclic ligand having thioether groups as coordinating agents.

Experimental Part

Unless specifically mentioned, all operations were performed under nitrogen atmosphere. Dehydrated and deoxygenated solvents were used to synthesize the ligands. MeOH was dehydrated with Mg, and benzene with Na/benzophenone. Solvents were placed under vacuum to eliminate the dissolved oxygen. In all cases this treatment was sufficient to operate the reaction. Sodium methoxide had been prepared from sodium metal

* To whom all correspondence should be addressed.
† Universitat Autônoma de Barcelona.
‡ Institut "Jaume Almera".

